

cal chemical, electronic, and structural changes are monitored in situ as a function of imposed environmental conditions. These types of studies may well be the trend in the distant future; however, in the near future it is anticipated that the bulk of the studies will be on model systems in order that the full potential of quantification can be assessed.

References and Notes

1. V. F. Weisskopf, *Science* **203**, 240 (1979).
2. J. Hillier and R. F. Baker, *J. Appl. Phys.* **15**, 663 (1944).
3. See, for example, A. V. Crewe, N. Isaacson, D. E. Johnson, *Rev. Sci. Instrum.* **42**, 411 (1971); J. R. Fields, *Ultramicroscopy* **21**, 311 (1977).
4. A. V. Crewe, *Optik* **47**, 299 (1977).
5. S. T. Manson, *Phys. Rev. A* **6**, 1013 (1972).
6. R. D. Leapman, P. Rez, D. Mayers, *Proc. 9th Int. Congr. Electron Microsc.* **1**, 526 (1978).
7. D. C. Joy and D. M. Maher, *Proc. 10th Annu. Scanning Electron Microsc. Symp.* **1**, 325 (1977).
8. J. A. Venables and A. P. Janssen, *Proc. 9th Int. Congr. Electron Microsc.* **3**, 280 (1978).
9. M. Isaacson and D. E. Johnson, *Ultramicroscopy* **1**, 33 (1975).
10. R. E. Watson and M. L. Perlman, *Science* **199**, 1295 (1978).
11. M. Isaacson and M. Utlaut, *Optik* **50**, 213 (1978).
12. See the data in (11) and also in K. O. Hodgson and S. Donach, *Chem. Eng. News* **56**, 26 (21 August 1978).
13. J. P. Blewett, Ed., *Brookhaven Natl. Lab. Rep. BNL 50595* (1977).
14. C. Colliex and P. Trebbia, in *Biological X-ray Microanalysis by Electron Beam Excitation*, C. Lechene and R. Warner, Eds. (Academic Press, New York, 1979).
15. J. L. Costa, D. C. Joy, D. M. Maher, K. L. Kirk, S. W. Hui, *Science* **200**, 537 (1978).
16. This sample of synaptosomes containing fluorodopamine was prepared by freeze substitution and supplied by J. L. Costa.
17. M. Isaacson, in *Proceedings of a Specialist Workshop on Analytical Electron Microscopy*, J. Silcox and M. Isaacson, Eds. (Materials Research Center, Cornell University, Ithaca, N.Y., 1977), p. 66.
18. J. L. Costa, D. M. Maher, D. C. Joy, unpublished data.
19. R. F. Egerton, *Proc. 11th Annu. Scanning Electron Microsc. Symp.* **1**, 13 (1978).
20. R. D. Leapman, *Ultramicroscopy* **3**, 413 (1978); see also (5, 6).
21. R. F. Egerton, in *Proceedings of a Specialist Workshop on Analytical Electron Microscopy*, P. L. Feyes, Ed. (Report 3082, Materials Research Center, Cornell University, Ithaca, N.Y., 1978), p. 232.
22. D. C. Joy, R. F. Egerton, D. M. Maher, *Proc. 12th Annu. Scanning Electron Microsc. Symp.* **2**, 817 (1979).
23. C. Jeanguillaume, P. Trebbia, C. Colliex, *Ultramicroscopy* **3**, 237 (1978).
24. D. C. Joy and D. M. Maher, in *Advances in Electron Microscopy and Analysis*, D. L. Misell, Ed. (Institute of Physics, London, 1978), p. 69.
25. J. L. Costa, D. C. Joy, D. M. Maher, in preparation.
26. K. I. Kirk, *J. Heterocyclic Chem.* **13**, 1253 (1976).
27. These images, of air-dried human blood platelets incubated with fluoroserotonin, are from unpublished work; they are reproduced here by courtesy of S. W. Hui and P. Ottensmeyer.
28. M. Isaacson, *J. Chem. Phys.* **56**, 1813 (1972).
29. D. E. Johnson, *Radiat. Res.* **49**, 63 (1972).
30. C. Colliex and B. Jouffrey, *Philos. Mag.* **25**, 191 (1972).
31. R. F. Egerton and M. J. Whelan, *J. Electron. Spectrosc. Relat. Phenom.* **3**, 232 (1976).
32. ———, *Philos. Mag.* **30**, 739 (1976).
33. C. Colliex, in *Seminar-Benchit Kontron, Analytische Elektronenmikroskopie* (Kontron, Munich, 1976), p. 204; see also C. Colliex, V. E. Cosslet, R. D. Leapman, P. Trebbia, *Ultramicroscopy* **1**, 301 (1976).
34. J. J. Ritsko, N. O. Lipari, P. C. Gibbons, S. E. Schnatterly, *Phys. Rev. Lett.* **37**, 1068 (1976).
35. B. M. Kincaid, A. E. Meixner, P. M. Platzman, *ibid.* **40**, 1296 (1978).
36. J. J. Ritsko and R. W. Bigelow, *J. Chem. Phys.* **69**, 4162 (1978).
37. S. G. Slusky, P. C. Gibbons, S. E. Schnatterly, J. R. Fields, *Phys. Rev. Lett.* **36**, 326 (1976).
38. R. D. Leapman and J. Silcox, *ibid.* **42**, 1361 (1979).
39. J. Kessler, *Polarized Electrons* (Springer-Verlag, New York, 1976).
40. For example, see K. Siegbahn *et al.*, *ESCA Applied to Free Molecules* (North-Holland, Amsterdam, 1969), p. 104.
41. F. Donoyer, R. Comis, A. F. Garito, A. J. Heeger, *Phys. Rev. Lett.* **35**, 445 (1975).
42. P. E. Eisenberger, in *Proceedings of the Robert A. Welch Foundation Conference on Chemical Research, XIX. Photon Chemistry*, W. O. Milligan, Ed. (Welch Foundation, Houston, 1975), p. 171.
43. J. J. Ritsko, S. E. Schnatterly, P. C. Gibbons, *Phys. Rev. Lett.* **32**, 671 (1974).
44. R. D. Leapman and V. E. Cosslet, *J. Phys. D* **9**, 25 (1976).
45. R. de L. Kronig, *Z. Phys.* **70**, 317 (1931); *ibid.* **75**, 191 (1932); *ibid.*, p. 468.
46. P. Eisenberger and B. M. Kincaid, *Science* **200**, 1441 (1978).
47. P. A. Lee and G. Beni, *Phys. Rev. B* **15**, 2862 (1977).
48. A. E. Meixner and G. S. Brown, *Rev. Sci. Instrum.*, in press.
49. P. E. Batson, in *Proceedings of a Specialist Workshop on Analytical Electron Microscopy*, P. L. Feyes, Ed. (Report 3082, Materials Research Center, Cornell University, Ithaca, N.Y., 1978), p. 31; also see *Ultramicroscopy* **3**, 367 (1978); P. E. Batson and A. J. Craven, *Phys. Rev. Lett.* **42**, 893 (1979).

Precision Optical Testing

James C. Wyant

During the 1960's new optical testing techniques began to develop with the introduction of the laser. At that time, also, the computer became important in the analysis of optical testing results.

so that atmospheric turbulence would not affect the results. Now with the availability of rapid, low-cost data reduction, large optics can be tested many times in the presence of atmospheric tur-

Summary. Increased performance requirements for modern optical systems have necessitated the development of more precise optical testing techniques. The need for accurate and rapid measurements is being met by the use of laser interferometers, microprocessors to gather test data, and computers to analyze the data and remove errors in the test equipment.

Today, with the introduction of more powerful minicomputers and microprocessors, vast improvements are being made in both the quality of optical testing and the cost. Formerly, large vacuum tanks were required to test large optics

bulence, and the results can be averaged to reduce the effects of turbulence.

Computers are also beginning to play an important role in reducing the quality of accessory optics used in an optical test. Formerly, all accessory optics had

to be of better quality than the optics under test. Now it is almost a routine matter to calibrate the quality of accessory optics and subtract the test errors in the data analysis of the test result.

This article first describes classical optical testing techniques, and then the basic interferometric testing techniques, with emphasis on laser techniques. New techniques made possible by the use of computers and microprocessors are also described.

Testing Techniques

Three noninterferometric testing techniques are the Foucault knife-edge test, the Ronchi test, and the Hartmann test. Before looking at these tests, let us look at what an optical test should measure.

Ideally, light coming from a single object point should, after reflection off a mirror or transmission through a lens, be focused to a perfect point. However, because light travels as a wave, it never comes to a perfect point focus, but rather is spread over some area. This spread is known as the point image irradiance distribution. For a perfectly designed and

The author is a professor of optical sciences at the Optical Sciences Center, University of Arizona, Tucson 85721.

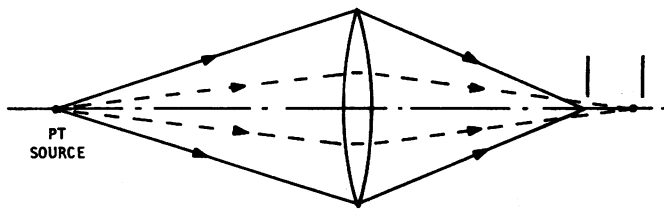


Fig. 1 (left). Different zones of a lens focus light at different positions. The parallel lines at the right indicate aberration.

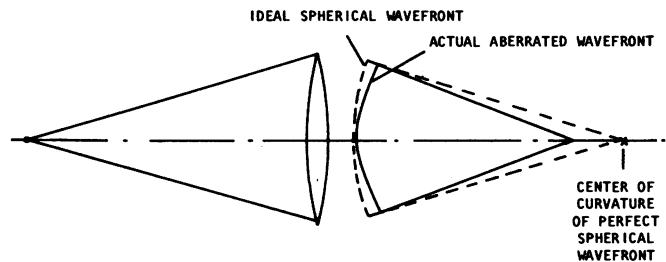


Fig. 2 (right). Lens produces aberrated wavefront rather than perfect spherical wavefront.

fabricated lens or mirror, the irradiance distribution of the image of a point source is called the aberration-free point spread function. If the optics are not perfect, the light going through different regions of a lens will come to focus at different positions, thus spreading over a larger area (Fig. 1).

To ensure that the light rays passing through all regions of the lens must come to focus at the same spot, it is necessary to know which portions of the lens are too thick and by how much, so that corrections can be made.

The wavefront of the light after it passes through the lens must be known. By wavefront is meant the shape of the surface for which the travel time for light leaving the source and arriving at the surface is a constant. The perfect wavefront shape after light passes through the

lens is a spherical one whose center of curvature is at the image position. The difference between the actual and the spherical wavefronts (Fig. 2) indicates the thickness error in the lens. The purpose of optical testing is to determine the difference between the actual wavefront shape and the perfect wavefront shape.

In classical testing techniques it is not possible to measure the wavefront directly, but rather the slope of the wavefront is measured. For example, in the Foucault knife-edge test (1) first described in 1858, a knife edge placed in the image plane is passed through the image of a point source (Fig. 3). The observer's eye is placed immediately behind the knife edge and focuses on the optics being tested. As the knife edge passes through the image, a shadow is

seen to pass across the aperture of the optics being tested. The more compact the light distribution in the image, the more rapidly the shadow passes the aperture.

A perfect lens will have one image point such that the entire aperture of the lens is seen to darken almost instantaneously when the knife edge is passed through the image. If the knife edge is moved longitudinally toward the lens from this image point and again passed through the image, the shadow will be seen to travel across the aperture in the same direction in which the knife edge is passed through the image (Fig. 3). When the knife edge is located behind the point image, the opposite motion of the shadow occurs. The ultimate sensitivity of the test is attained from the motion of the shadow within certain zones of the aper-

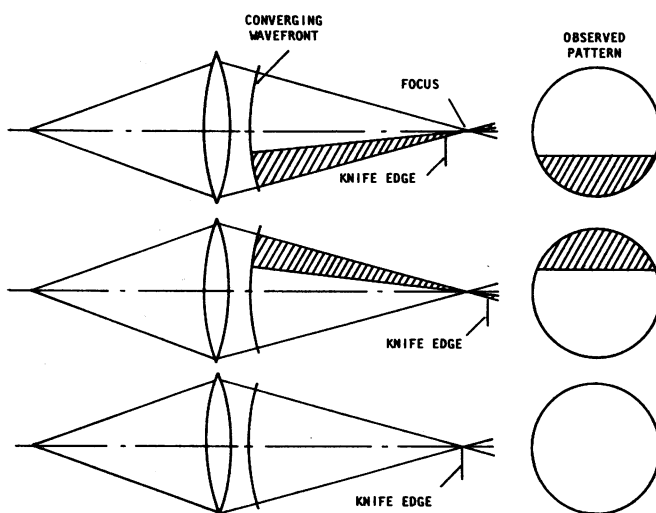
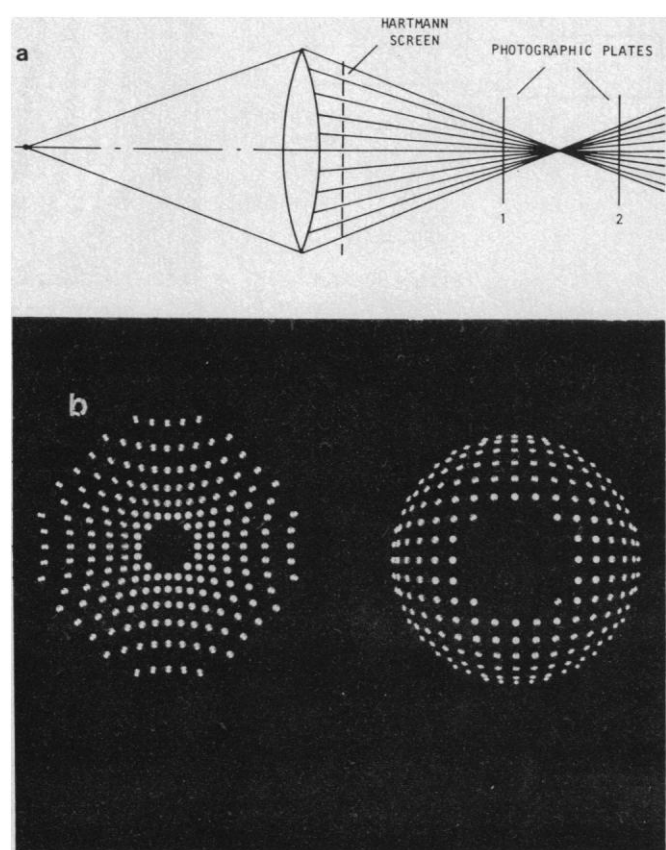


Fig. 3 (left above). Foucault knife-edge test.



INSIDE FOCUS

OUTSIDE FOCUS

ture as the knife edge cuts through the image. In practice, the knife edge is most often used to measure the focal position of different parts of the optical element being tested. This information reveals where the high and low parts of a surface are.

In the classical Ronchi test (2) first described in 1923, a series of opaque and transparent lines called a Ronchi ruling are substituted for the knife edge used in the Foucault test. Each line in the Ronchi ruling produces a shadow just as the knife edge produces a shadow in the Foucault test. Since several positions of the knife edge are present simultaneously, it is not necessary to move the edges through the image.

A third noninterferometric test commonly used by astronomers is the Hartmann test (3). For this test a plate containing an array of holes is placed in a converging beam of light produced by the optics under test. One or more photographic plates are successively placed in the converging light beam after the Hartmann screen as shown in Fig. 4a. The positions of the images of the holes in the screen as recorded on the photographic plates and illustrated in Fig. 4b give the wavefront slope errors.

Interferometers

In most current high-precision optical tests interferometric techniques are used. One of the most commonly used interferometers is the Twyman-Green interferometer (Fig. 5) for testing a flat mirror. Generally a laser is used as the light source. The laser beam is expanded to match the size of the sample being tested. Part of the laser light is transmitted to the reference surface and part is reflected by the beamsplitter to the flat surface being tested. Both beams are reflected back to the beamsplitter where they are combined to form interference fringes. An imaging lens projects the surface under test onto the observation plane.

Fringes (Fig. 6) show defects in the surface being tested. If the surface is perfectly flat, straight, equally spaced fringes are obtained. Departure from the straight, equally spaced condition shows directly how the surface differs from being perfectly flat. For a given fringe, the difference in optical path between light going from laser to reference surface to observation plane and the light going from laser to test surface to observation plane is a constant. (The optical path is equal to the product of the geo-

metrical path times the refractive index.) Between adjacent fringes (Fig. 6) the optical path difference changes by one wavelength, which for a helium-neon laser corresponds to 633 nm. The number of straight, equally spaced fringes and their orientation depend upon the tip-tilt of the reference mirror. That is, by tipping or tilting the reference mirror the difference in optical path can be made to vary linearly with distance across the laser beam.

Deviations from flatness of the test mirror also cause optical path variations. A height change of half a wavelength will cause an optical path change of one wavelength and a deviation from fringe straightness of one fringe. Thus, the fringes give us surface height information just as a topographical map gives us height or contour information.

The existence of the essentially straight fringes provides a means of measuring surface contours relative to a tilted plane. This tilt is generally introduced to indicate the sign of the surface error, that is, whether the errors correspond to a hill or a valley. One way to get this sign information is to push in on the piece being tested when it is in the interferometer. If the fringes move toward the right when the test piece is pushed toward the beamsplitter, then fringe deviations from straightness toward the right correspond to high points (hills) on the test surface and deviations to the left correspond to low points (valleys).

For example, the basic Twyman-Green interferometer (Fig. 5) can be modified (Fig. 7) to test concave spherical mirrors (4). In the interferometer, the center of curvature of the surface under test is placed at the focus of a high quality diverger lens so that the wavefront is reflected back onto itself. After this retroreflected wavefront passes through the diverger lens it will be essentially a plane wave, which, when it interferes with the

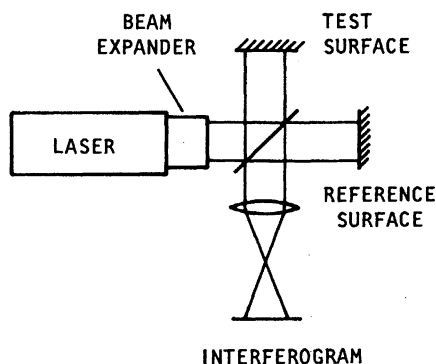


Fig. 5. Twyman-Green interferometer for testing flat surfaces.

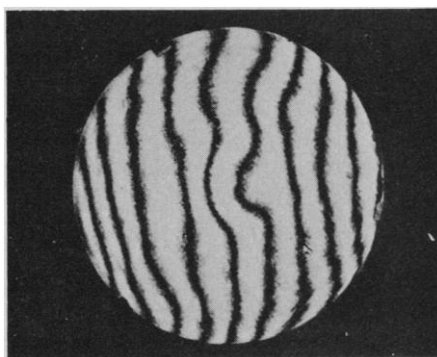


Fig. 6. Interferogram obtained with the use of a Twyman-Green interferometer to test a flat surface.

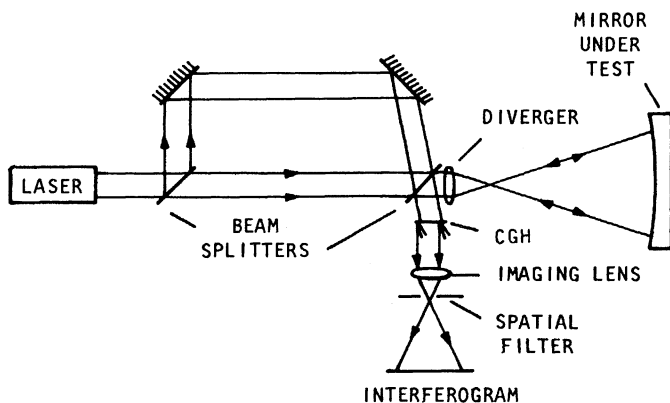


Fig. 7 (left). Twyman-Green interferometer for testing spherical mirrors or lenses. used for computer-generated hologram testing of aspherics.

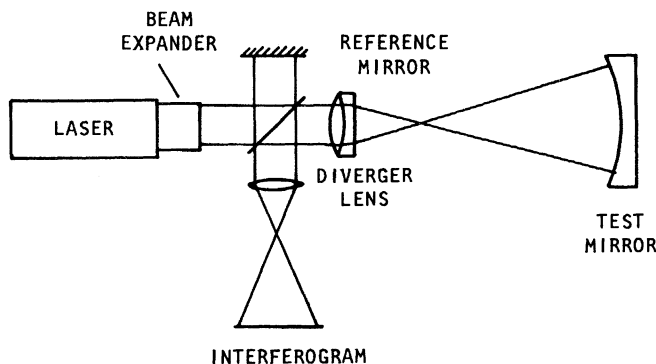


Fig. 8 (right). Modified Twyman-Green interferometer

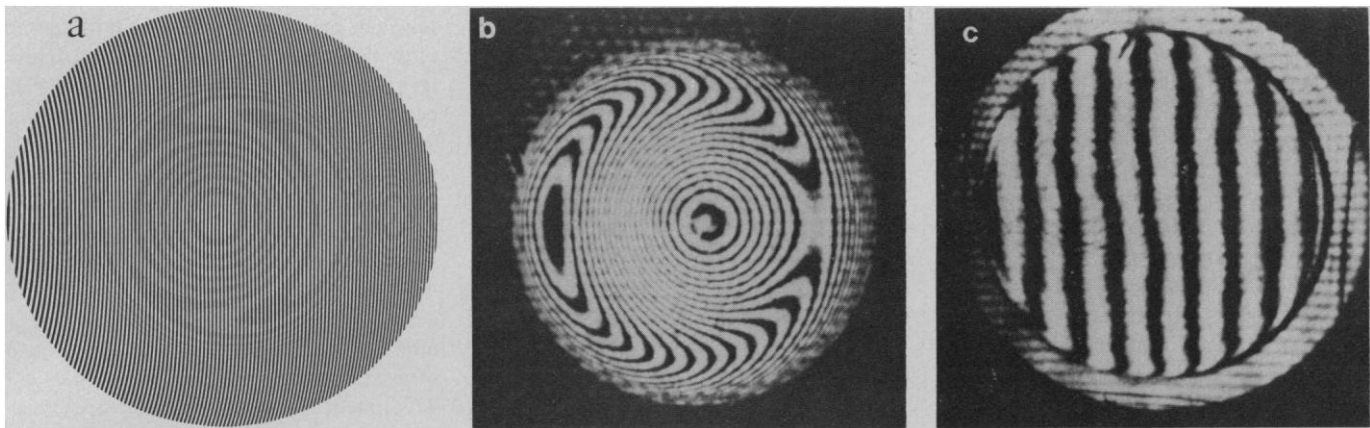


Fig. 9. (a) Computer-generated hologram, (b) interferogram obtained testing a parabolic mirror without CGH, and (c) interferogram obtained testing a parabolic mirror with a CGH.

plane reference wave, will give interference fringes similar to those shown above for testing flat surfaces. In this case it indicates how the concave spherical mirror differs from the desired shape. Likewise, a convex spherical mirror can be tested. Also, if a high-quality spherical mirror is used, the high-quality diverger lens can be replaced with the lens to be tested.

There is much interest in the use of aspheric surfaces in optical systems. Often the use of aspheric surfaces can improve system performance and reduce the number of optical components required. If the Twyman-Green interferometer (as well as other types) is used to test an aspheric surface, the resulting interferogram will be complicated even if the surface under test is perfect. The problem is that the interferometer provides a null test; that is, straight, equally spaced fringes are obtained only when spherical surfaces are tested. To overcome this problem the regular diverger lens, which produces a good spherical wavefront, can be replaced with a diverger lens that produces a wavefront that will match the aspheric surface being tested when it is perfect. This new diverger lens is called a null lens since it will give null, or equally spaced straight fringes when the aspheric surface under test is perfect. A problem with null lenses is that they can be expensive, and a separate null lens must be made for each different aspheric surface tested.

A second way of modifying a Twyman-Green interferometer to test aspheric wavefronts is to use a computer-generated hologram (CGH) (5). When a CGH is used to test aspherics, the interferometer is first computer-ray traced to find the ideal interferogram, which would be obtained if the aspheric surface under test were perfect. This interferogram is then drawn by a computer-

controlled plotter. If it is not drawn to the proper size it must undergo photoreduction to the proper size before it is placed in the interferometer (Fig. 8). When this interferogram, or hologram, as it is more generally called, is illuminated with the plane reference wave, it produces a wavefront identical to the wavefront coming from the aspheric element under test if it is perfect. Other wavefronts are also produced, but they leave the holograms at different angles and will not pass through the small-aperture spatial filter placed between the lens and the interferogram. The interference of this reference wavefront and the wavefront from the aspheric surface under test shows how the surface being tested departs from the desired aspheric shape. If the aspheric surface under test is perfect, straight, equally spaced fringes are obtained.

Figure 9a shows a CGH made to test an aspheric mirror, in this case a parabolic mirror. Figure 9b shows the interferogram obtained by means of the Twyman-Green interferometer without the CGH to test the parabolic mirror, and Figure 9c shows the interferogram ob-

tained with the CGH. (The CGH shown in Fig. 9a was not used to obtain the results shown in Fig. 9c. The lines in the CGH used in obtaining Fig. 9c are too closely spaced to make a good illustration.) While the interferogram obtained without the CGH is hard to analyze, the interferogram obtained using the CGH clearly shows that the parabolic mirror has nearly the correct shape.

The main advantages of using a CGH to test aspheric surfaces are that they produce a null test that is easy to interpret, and the surface error can be measured directly for the entire surface. Furthermore, once the computer software is written for producing a CGH and the necessary computer-controlled plotter is obtained, it is relatively inexpensive and fast to produce a CGH.

Applications of Computers

The computer generation of holograms to test aspheric surfaces is but one of the many uses of computers in precision optical testing. The most widespread use is for the analysis of interferograms (6). In-

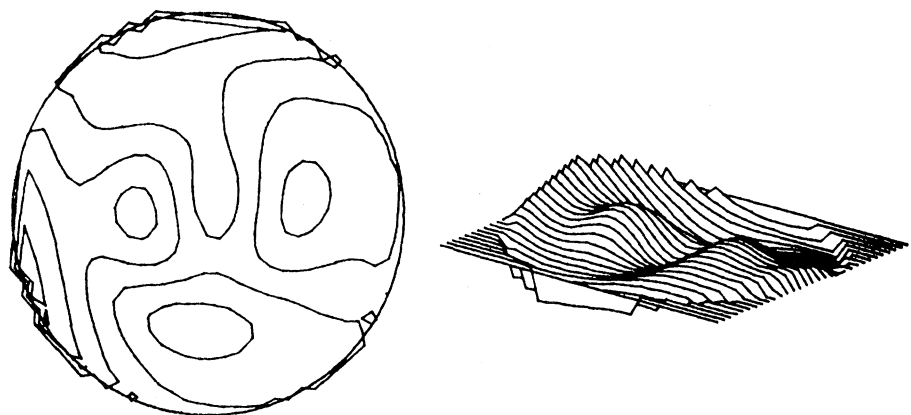


Fig. 10. Computer-calculated contour map having a contour step of 0.1 wave per fringe and the associated three-dimensional wavefront plot.

terferograms are first scanned with a comparator or digitization tablet to locate the fringe centers. Computer software then fits this fringe center location to a set of polynomials to determine the aberrations present. While the change in the difference of the optical path between fringes on the interferogram is one wave, the computer can use the derived polynomials to draw a contour map showing what the interferogram would look like at other contour levels, such as 0.1 wave per fringe. The tilt of the reference plane can be varied to make the interferogram clearer at smaller contour levels. Known aberrations in the test setup can be removed, and a contour map or interferogram can be drawn to show only the errors in the optics tested. If noise is produced by atmospheric turbulence, several interferograms can be averaged to reduce the noise, and an average contour map can be drawn. Also, three-dimensional plots can be drawn to aid in the visual interpretation of the surface errors. Figure 10 shows a typical computer-calculated contour map and a three-dimensional plot.

Once the interferogram fringe centers are fit with polynomials, the performance of the optical system can be calculated. For example, the image of a perfect point source can be determined and plotted. Specific amounts of aberrations are calculated and the amount of energy in the image as a function of area can also be calculated. Spot diagrams that show the image position for different light rays through the system can be plotted. And the modulation transfer function, which is a quantitative description of image detail as a function of size of the detail in the object, can be calculated, as well as a host of other important quantities.

As mentioned above, interferograms are generally scanned by hand to deter-

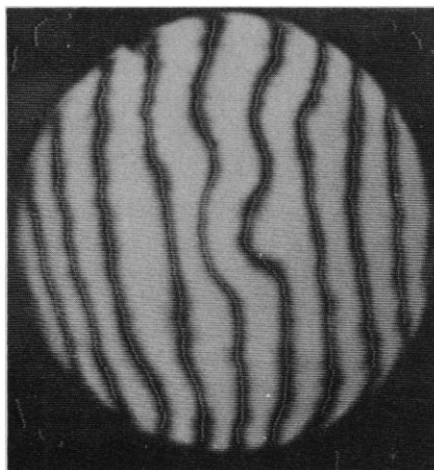


Fig. 11. Interferogram automatically scanned by use of a TV system and microprocessor to determine fringe centers.

mine fringe centers, although methods of automation are being studied. Television systems can be used to scan the interferogram (7) for "live" interference fringes as well as photographs of fringes. A microprocessor can then be used to determine the fringe centers (Fig. 11). If manual scanning were used to determine fringe centers, probably only 20 to 30 points along a fringe would be determined. The microprocessor, however, works so rapidly and easily that many more fringe centers can be determined. For the example shown in Fig. 11, 480 points along a fringe were measured and stored in less than 5 seconds. This time could be decreased if desired.

Another electronic technique for automatically scanning interference fringes is called AC, heterodyne, or in some instances digital, interferometry. For this technique, the difference in optical path between the two interfering beams in the interferometer is varied in a known manner either in discrete steps or continuously (8). Several electrooptic modula-

tors can produce this variation in optical path difference. If the optical path difference between the two beams varies continuously at a constant rate, the intensity at any given point in the interference pattern varies sinusoidally with time. An electronic light detector placed at a point in the interferogram will give a sinusoidal output whose phase indicates the desired wavefront information at the detector point. Since electronic techniques for precisely measuring the phase of a sinusoidally varying signal are well developed, a square array of detectors in the interference pattern can yield the wavefront data desired. These wavefront data can then be analyzed in the same manner as the data from more conventional interferograms. Interferometers of this type have been constructed to take data at kilohertz or higher rates. Thus an enormous amount of data can be gathered to reduce noise effects and to obtain surface data correct to a few angstroms with less precise test setups than previously required. Without a doubt, microprocessors will continue to revolutionize optical testing for many more years.

References and Notes

1. L. M. Foucault, *C.R. Acad. Sci. Paris* **47**, 958 (1858).
2. V. Ronchi, *Riv. Ottica Mecc. Precis.* **2**, 9 (1923).
3. J. Hartmann, *Z. Instrumentenk.* **20**, 47 (1900).
4. J. B. Houston, C. J. Buccini, P. K. O'Neill, *Appl. Opt.* **6**, 1237 (1967).
5. J. C. Wyant, in *Optical Shop Testing*, D. Malacara, Ed., (Wiley, New York, 1978), pp. 389-397.
6. J. S. Loomis, in *Optical Interferograms—Reduction and Interpretation*, A. H. Guenther and D. H. Liebenberg, Eds. (American Society for Testing and Materials, Philadelphia, Pa., 1978), pp. 71-86.
7. K. Womack, J. Jonas, C. Koliopoulos, K. Underwood, J. Wyant, J. Loomis, C. Hayslett, in *Interferometry*, G. Hopkins, Ed. (SPIE Proceedings 192, Society of Photo-Optical Instrumentation Engineers, Bellingham, Wash., in press).
8. J. C. Wyant, in *Optica Hoy Y Mañana*, J. Bescos et al., Eds. (Proceedings of the Eleventh Congress of the International Commission for Optics, 1978), pp. 659-662.